

# Influence of Particle Size and Polymer–Filler Coupling on Viscoelastic Glass Transition of Particle-Reinforced Polymers

C. G. Robertson,<sup>\*,†</sup> C. J. Lin,<sup>†</sup> M. Rackaitis,<sup>†</sup> and C. M. Roland<sup>‡</sup>

Bridgestone Americas, Center for Research and Technology, 1200 Firestone Parkway, Akron, Ohio 44317-0001, and Chemistry Division, Code 6120, Naval Research Laboratory, Washington, D.C. 20375-5342

Received October 6, 2007; Revised Manuscript Received January 22, 2008

**ABSTRACT:** The viscoelastic glass-to-rubber softening transition is analyzed for various cross-linked polymers reinforced with filler particles. We find that the loss modulus peak corresponding to the segmental relaxation process (glass transition) is not significantly affected by the particle surface area in carbon black-filled polybutadiene or by silane chemical coupling of poly(styrene-*co*-butadiene) to silica. Large differences in shape and magnitude of the peak in the loss tangent ( $\tan \delta$ ) vs temperature are noted for these materials; however, this is due to variations in the storage modulus at small strains in the rubbery state, which is influenced by the nature of the jammed filler network. The use of a simple relaxation model demonstrates this feature of the viscoelastic glass transition in filled rubber. It is not necessary to invoke concepts involving a mobility-restricted polymer layer near the filler surfaces to explain the viscoelastic results. Atomic force microscopy conducted with an ultrasharp tungsten tip indicates that there may be some stiffening of the elastomer in the proximity of filler particles, but this does not translate into an appreciable effect on the segmental dynamics in these materials.

## Introduction

Despite significant research activity on the effect of nanoscale confinement on the glass transition temperature ( $T_g$ ) of polymers, many controversial issues remain unresolved, as recently reviewed by Alcoutlabi and McKenna.<sup>1</sup> Of particular relevance to the field of elastomers is the influence of reinforcing particles on the polymer  $T_g$ . It is reasonable to expect that physical adsorption or chemical attachment of polymer chains to rigid particles can slow down the polymer dynamics, which might increase the glass transition of the polymer chains near particle surfaces. However, while some published studies show increases in  $T_g$  upon the addition of carbon black, silica, or other fillers, others report no change in  $T_g$  or even  $T_g$  decreases.<sup>2–26</sup> The nature of the interfacial interactions between the polymer and particles may account for some of the disparate results concerning the effect of fillers on  $T_g$ .<sup>15,27</sup>

From techniques such as nuclear magnetic resonance,<sup>18–21</sup> dielectric spectroscopy,<sup>22,23</sup> and neutron scattering<sup>24–26</sup> which directly probe polymer molecular motions, there is evidence that the segmental relaxation of some portion of polymer chains can be retarded by filler particles. The extent to which these localized effects translate into modification of the viscoelastic  $T_g$  of the bulk polymer is unclear. Dynamic mechanical testing is often employed to study the impact of particles on the  $T_g$  of polymers,<sup>2–11</sup> but many of these studies draw conclusions based on the isochronal loss tangent ( $\tan \delta = G''/G'$ ) vs temperature peak that occurs near the glass transition. This can be problematic because  $\tan \delta$  in the glass-to-rubber softening region is influenced not only by local segmental motions, as reflected in the loss modulus ( $G''$ ) toward lower  $T$ , but also by filler reinforcement effects on both the storage modulus ( $G'$ ) and  $G''$  at higher  $T$ . In this paper we illustrate this through detailed viscoelastic characterization of carbon black-filled polybutadiene and poly(styrene-*co*-butadiene) reinforced with silica particles. The impact of the degree of particle–polymer interaction on the dynamic mechanical properties in the glass transition region is probed by studying carbon blacks with widely varying particle

size and surface area and by the use of both a filler–filler shielding additive and a polymer–filler coupling agent in the silica-filled compounds.

## Experimental Details

A poly(styrene-*co*-butadiene) statistical copolymer (Duradene 715 from Firestone Polymers, LLC), commonly referred to as styrene–butadiene rubber (SBR), was mixed with precipitated silica and cured to form a filled rubber. The characteristics of this SBR are given elsewhere.<sup>28</sup> The silica used was HiSil 190 from PPG Industries, Inc., which has specific surface area in the range from 200 to 210 m<sup>2</sup>/g. This particular grade of precipitated silica was studied in detail by Schaefer et al.<sup>29</sup> using a variety of scattering and microscopy techniques. The formulation, mixing conditions, and curing procedure are identical to those reported in the recent study by Scurati and Lin<sup>28</sup> (compound category III) with the exception of the amounts of filler–filler shielding agent (*n*-octyltriethoxysilane) and polymer–filler coupling agent (3-mercaptopropyltrimethoxysilane). In the present study, one sample had no coupling agent or shielding agent, one sample had 6.5% shielding agent, and one sample had 4.7% coupling agent (weight basis, relative to polymer amount). The silica volume fractions in these three compounds were very similar at values of 0.21, 0.20, and 0.20, respectively. We also studied polybutadiene elastomers filled with carbon black particles of various types at a constant filler volume fraction of 0.18. Details about the polybutadiene, rubber formulation, mixing procedures, and curing conditions for these materials were previously reported.<sup>30</sup>

The viscosities of the uncured rubbers were evaluated at 130 °C in a Mooney viscometer using the large rotor. Bound rubber, which is the percentage of polymer not extracted by solvent from the uncured sample, was measured by immersion in an excess of toluene at 23 °C for 3 days, followed by filtering, drying, and weighing.

Oscillatory shear testing was performed on a TA Instruments ARES (200 and 2000 g-cm force rebalance transducers). The temperature dependence of the viscoelastic response was determined at a constant strain amplitude ( $\gamma$ ) of 0.25%. The temperature was changed incrementally, with the sample equilibrated at each temperature before testing; this maintains thermal equilibrium during all data acquisition unlike the more usual nonisothermal, temperature ramp experiment. Isothermal strain sweeps were also performed in which the strain amplitude was increased in logarithmic

\* Corresponding author: e-mail [chris99robertson@yahoo.com](mailto:chris99robertson@yahoo.com).

<sup>†</sup> Bridgestone Americas, Center for Research and Technology.

<sup>‡</sup> Naval Research Laboratory.

**Table 1. Characteristics of Carbon Blacks<sup>a</sup>**

carbon black type	$d$ (nm)	$D$ (nm)	$S$ (m <sup>2</sup> /g)
N110	17 ± 7	54 ± 26	143
N220	21 ± 9	65 ± 30	117
N351	31 ± 14	89 ± 47	75
N550	53 ± 28	139 ± 71	41
N660	63 ± 36	145 ± 74	34
N762	110 ± 53	188 ± 102	21
N990	246 ± 118	376 ± 152	9

<sup>a</sup> Values for primary particle diameter ( $d$ ), particle aggregate diameter ( $D$ ), and specific surface area ( $S$ ) are from Hess and McDonald.<sup>31</sup>

steps from 0.03 to 6%. All of the dynamic mechanical measurements were conducted using a frequency ( $\omega$ ) of 31.4 rad/s (5 Hz) and a torsion rectangular sample geometry. The reported strains are the values at the outer edge of the sample. The strain variation across the sample for this geometry has a small effect on the strain dependence of the softening (Payne effect) but does not impact the relative results for different compounds.

Atomic force microscopy was performed on the cross-linked polybutadiene sample filled with N351 carbon black. The equipment used was a Veeco (Digital Instruments) Dimension 3000 AFM with an ultrasharp tungsten tip by Mikromasch (nominal tip curvature radius is 1 nm). Measurements were conducted at room temperature. It was necessary to remove low-molecular-weight extractables (oil, wax, hydrocarbon resin, etc.) for the high-resolution tapping mode measurements with the ultrasharp tip. Samples were prepared by extraction of the rubber in toluene followed by drying under vacuum; the material removed amounted to less than 12 wt %. The surface was prepared by cryo-microtome, giving a surface roughness below 100 nm. Phase contrast images were collected in light tapping mode at a tapping amplitude equal to 85–90% of free oscillation amplitude.

## Results and Discussion

We studied polybutadiene filled with diverse types of carbon blacks, ranging from a highly reinforcing N110 grade with an aggregate diameter ( $D$ ) of about 50 nm to a N990 carbon black with  $D \approx 400$  nm and low reinforcement potential. The carbon black characteristics, as reported by Hess and McDonald,<sup>31</sup> are given in Table 1. This series of carbon blacks has a systematic variation in the particle surface area, a key aspect of the reinforcement of polymers with small particles. The Mooney viscosity and bound rubber measured for the uncured polybutadiene compounds reflect this varying degree of reinforcement (Figure 1). The amount of bound rubber depends on the solvent as well as the extraction time and temperature. For given

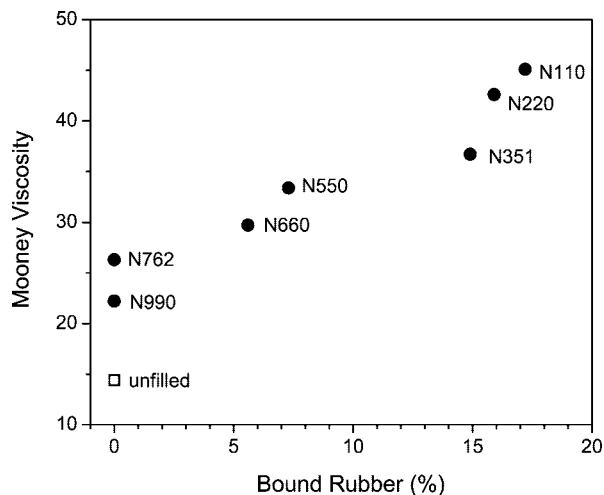


**Figure 1.** Mooney viscosity at 130 °C vs bound rubber for un-cross-linked polybutadiene, both unfilled and with the indicated carbon black types at a volume fraction of 0.18.

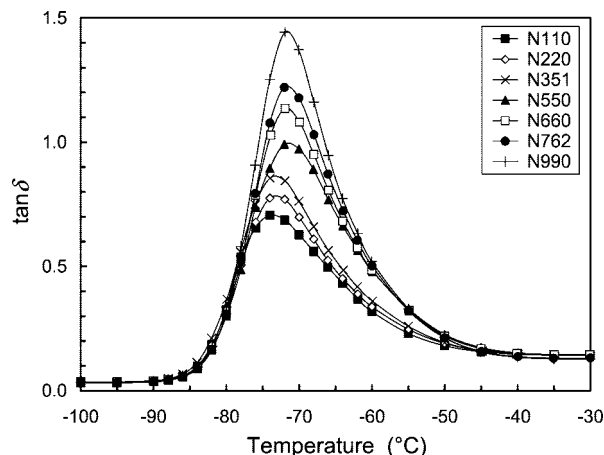


**Figure 2.** Temperature dependence of  $\tan \delta$  for polybutadiene with the indicated carbon black types at a constant filler volume fraction of 0.18. Measurements were made using  $\gamma = 0.25\%$  and  $\omega = 31.4$  rad/s.

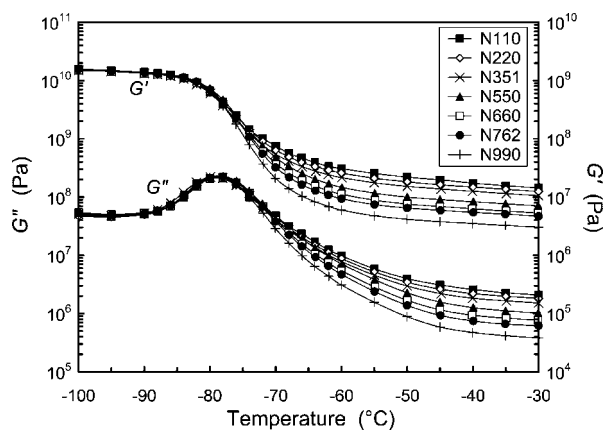


**Figure 3.** Plot of storage and loss moduli (logarithmic scale) vs temperature for polybutadiene reinforced with the indicated carbon black types at a constant filler volume fraction of 0.18. Measurements were made using  $\gamma = 0.25\%$  and  $\omega = 31.4$  rad/s. The axis scales for  $G'$  and  $G''$  have the same range but are offset for clarity.

conditions, the extent of bound rubber reflects the strength and extent of polymer–filler interactions.<sup>32,33</sup>

The large variation in shape and strength of the  $\tan \delta$  peaks for the rubber samples with the different carbon blacks (Figure 2) ostensibly suggests that the extent of interaction between polybutadiene and carbon black filler affects the glass transition; however, this is incorrect. The location and intensity of the  $G''$  peaks, which reflect only the segmental motion of the polybutadiene, are not appreciably influenced by the type of carbon black (Figures 3 and 4). As shown in Figure 3, carbon blacks with the larger surface areas yield more reinforcement above  $T_g$ . This reinforcement increases both  $G'$  and  $G''$  in the rubbery state, but the former is affected more due to the relatively low value of  $\tan \delta$  ( $\approx 0.15$ ) at temperatures above the glass-to-rubber softening transition. This is most easily observed using a linear scale for the moduli in Figure 4.

For the case of elastomers which contain precipitated silica, polymer–filler interactions can be controlled by (i) using a filler–filler shielding agent (*n*-octyltriethoxysilane) to promote less filler agglomeration and more contact between polymer and particles or (ii) introducing a polymer–filler coupling agent (3-mercaptopropyltrimethoxysilane) which creates sulfur linkages between the silica surface and the unsaturated polymer during mixing and vulcanization. We investigated the viscoelastic

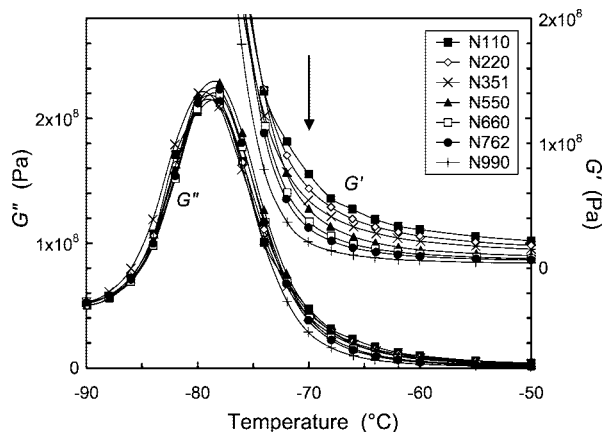


**Figure 4.** Plot of storage and loss moduli (linear scale) vs temperature for polybutadiene reinforced with the indicated carbon black types at a constant filler volume fraction of 0.18. Measurements were made using  $\gamma = 0.25\%$  and  $\omega = 31.4$  rad/s. The axis scales for  $G'$  and  $G''$  have the same range but are offset for clarity. The arrow marks the approximate position of the  $\tan \delta$  maxima.

response of SBR/silica compounds with either added shielding agent or coupling agent, in comparison to the behavior of the untreated compound. The results are presented in Figures 5 and 6. Similar to the data for the carbon black-filled polybutadiene, the  $G''$  peak, reflecting segmental motions, was essentially unaffected by changes in the polymer–filler interactions. Notable differences in the  $\tan \delta$  peaks were again observed and ascribed to increases in the stiffness of the rubber (polymeric chain modes) on the high-temperature side rather than to any changes in the segmental relaxation of the polymer.

To further illustrate the effect of rubbery modulus on the loss tangent peak, we use a simple relaxation model. We employ a single Maxwell element, modified to yield a finite modulus in the low-frequency limit (rubbery state), rather than the decay of  $G'$  and  $G''$  to zero. The storage and loss moduli in the rubbery state are represented by  $G'_R$  and  $G''_R$ , which are added to the Maxwell model expressions to give the following dependences on frequency:

$$G' = \frac{g(\omega\lambda)^2}{1 + (\omega\lambda)^2} + G'_R \quad (1)$$

$$G'' = \frac{g\omega\lambda}{1 + (\omega\lambda)^2} + G''_R \quad (2)$$

In the above expressions,  $\lambda$  is the relaxation time and  $g$  represents the relaxation strength. We vary  $G'_R$  but maintain the glassy modulus ( $G'_G$ ) at a constant value of  $1 \times 10^9$  Pa; hence,  $g$  must be adjusted according to

$$g = G'_G - G'_R \quad (3)$$

$G'_R$  and  $G''_R$  are related by

$$G''_R = \tan \delta_R G'_R \quad (4)$$

At low strains in the rubbery region above  $T_g$ , the filled cross-linked elastomers of interest herein have  $\tan \delta$  in the range from 0.1 to 0.2. In our model, we vary  $G'_R$  and use  $\tan \delta_R = 0.15$  to obtain  $G''_R$  from  $G'_R$ . We hold constant  $\lambda = 100$  s and  $G'_G = 1 \times 10^9$  Pa. The calculated dynamic mechanical spectra (Figure 7) show that the rubbery  $G'$  can govern the glass-to-rubber  $\tan \delta$  response, without changes in the loss modulus peak.

At sufficient filler concentration, the particles in an elastomer can form a percolated fractal network, yielding reinforcement well beyond the hydrodynamic effect. This particle network is progressively broken with increasing strain amplitudes in the

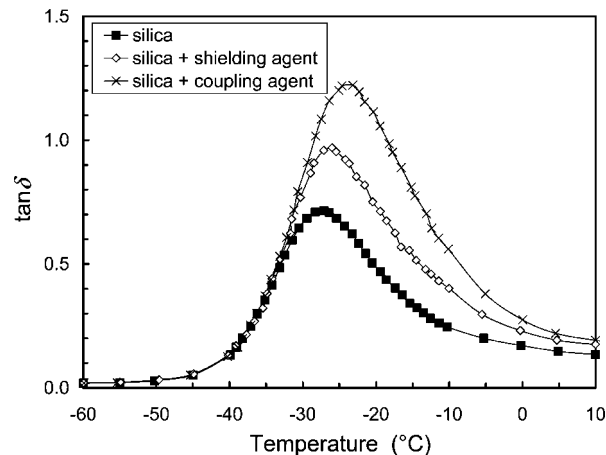


**Figure 5.** Temperature dependence of  $\tan \delta$  for SBR with a silica volume fraction of  $\sim 0.20$ . Measurements were made using  $\gamma = 0.25\%$  and  $\omega = 31.4$  rad/s.

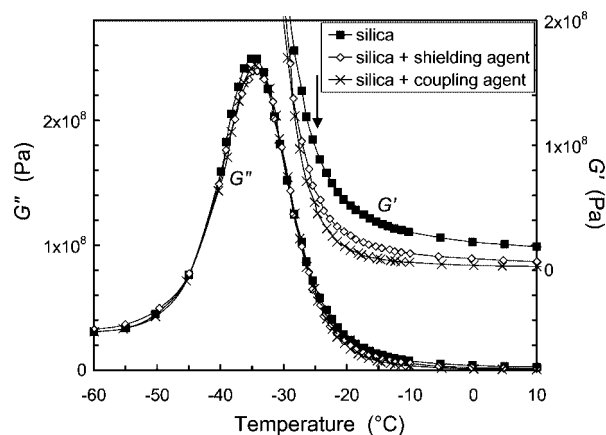


**Figure 6.** Plot of storage and loss moduli (linear scale) vs temperature for SBR with a silica volume fraction of  $\sim 0.20$ . Measurements were made using  $\gamma = 0.25\%$  and  $\omega = 31.4$  rad/s. The axis scales for  $G'$  and  $G''$  have the same range but are offset for clarity. The arrow marks the approximate position of the  $\tan \delta$  maxima.

range from 0.1 to 10%. The consequent reduction in modulus with strain amplitude is referred to as the Payne effect or an unjamming process.<sup>34–38</sup> The experimental glass-to-rubber softening results discussed thus far were all acquired using an oscillatory strain amplitude of 0.25%, at which disruption of the filler network is minimal. Higher strain (ca.  $\gamma = 10\%$ ) measurements across the glass transition range of the viscoelastic spectrum are difficult; in addition to possible instrumental compliance limitations, nonlinear yielding and associated local temperature rises in the sample preclude obtaining reliable data. However, the location of the maximum in  $\tan \delta$  is far enough above  $T_g$  (the peak in  $\tan \delta$  occurs 7 to 10 °C higher than the peak in  $G''$ ) to allow measurements to be conducted as a function of strain amplitude up to about 6% at this temperature. It can be noted from Figures 8 and 9 that the  $\tan \delta$  differences between compounds, seen in Figures 2 and 5, diminish as the particle networks are broken down with increasing  $\gamma$ . Thus, the small-strain damping behavior for these filled elastomers in the vicinity of the maximum in  $\tan \delta$  is dominated by the contribution from the jammed filler–filler network to the rubbery response.

Finally, we employ atomic force microscopy (AFM) using an ultrasharp tip in order to further examine the influence of particles on the local polymer mobility. The AFM tapping mode phase images for the polybutadiene with N351 carbon black are shown in Figure 10. There is some suggestion of stiffening (bright halo) in the rubber in close proximity to the particle

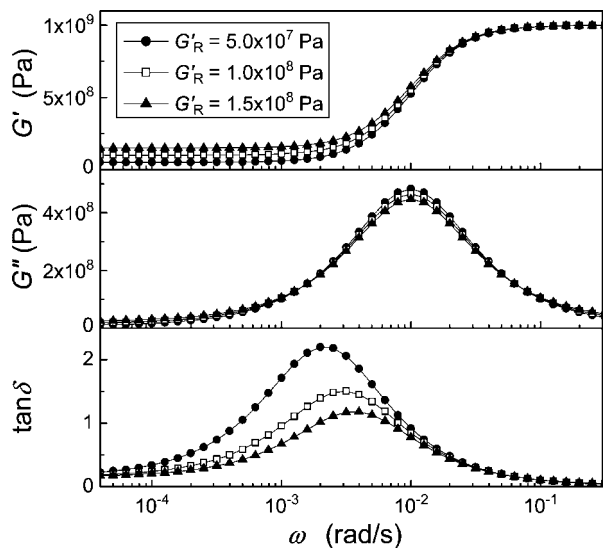


**Figure 7.** Calculated results for Maxwell model with values of rubbery modulus ( $G_R$ ) varied as shown. See text for additional information. For comparison with Figures 2–6, increasing  $T$  at fixed frequency would correspond to lower values of the abscissa.

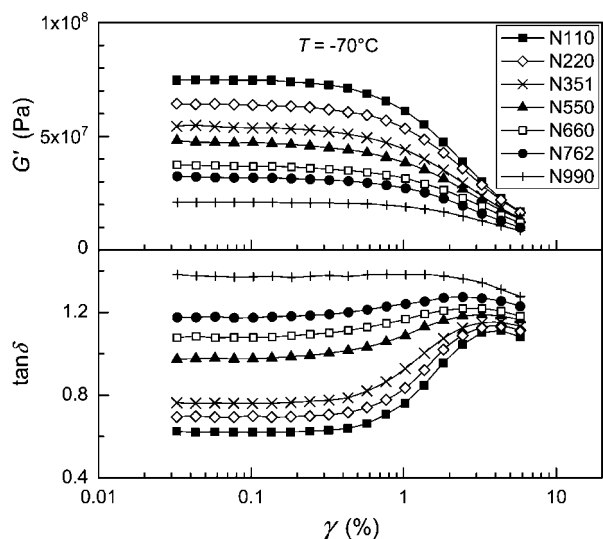


**Figure 8.** Strain amplitude dependence of  $G'$  and  $\tan \delta$  for polybutadiene with the indicated carbon black types at a constant volume fraction of 0.18. Measurements were made at  $T = -70$  °C using  $\omega = 31.4$  rad/s.

aggregates. However, this does not have a measurable effect on the bulk viscoelastic relaxation of the polymer, as evidenced by the invariance of the loss modulus peaks (reflecting segmental relaxation) both to large variations in particle surface area and to changes in polymer–filler coupling induced by additives.

### Final Comments

One example in the literature concerning the effect of particles on the polymer glass transition was given by Tsagaropoulos and Eisenberg.<sup>2,3</sup> This highly cited research showed the appearance of a second  $\tan \delta$  vs temperature peak in un-cross-linked polymers in the presence of nanosized silica filler. This peak, observed in some cases at temperatures as large as 100 °C above the main glass-to-rubber softening transition, was attributed to the glass transition of immobilized polymer chains near the particles. However, the temperature range of this putative “second glass transition” was in the region of the viscoelastic spectrum where the unfilled polymer exhibited

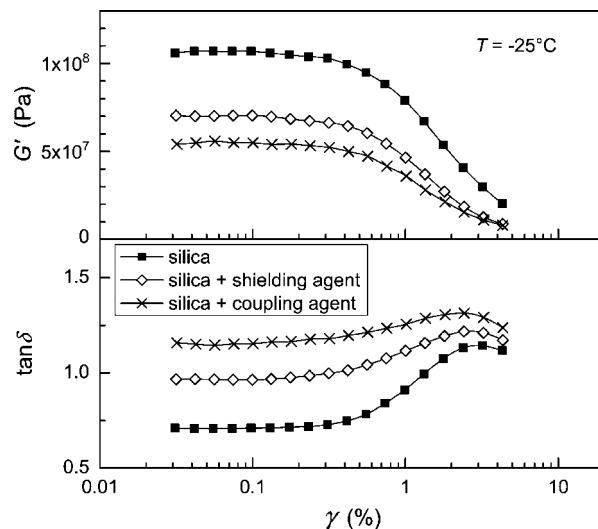


**Figure 9.** Strain amplitude dependence of  $G'$  and  $\tan \delta$  for SBR with a silica volume fraction of  $\sim 0.20$ . Measurements were made at  $T = -25$  °C using  $\omega = 31.4$  rad/s.

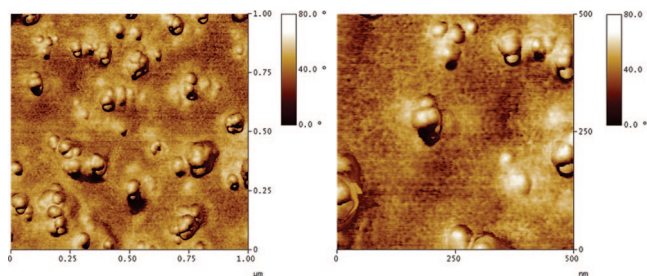


**Figure 10.** Tapping mode AFM images of polybutadiene with N351 carbon black. The scan size is  $1 \mu\text{m} \times 1 \mu\text{m}$  for the image on the left and  $500 \text{ nm} \times 500 \text{ nm}$  for the image on the right. The micrographs are phase contrast images, with softer regions appearing darker.

terminal flow; this suggests a different interpretation. Interaction of some polymer chains with filler would suppress their terminal relaxation process (chain diffusion), so that only unaffected chains would undergo relaxation in the normal temperature/frequency window; this would lead to a local peak in  $\tan \delta$  rather than the usual divergence of  $\tan \delta$  toward infinity as temperature is increased (or frequency is decreased). Such partial terminal flow has been demonstrated for bidisperse linear–linear blends and sparsely branched polymers,<sup>39–41</sup> for cross-linked polymer networks containing unattached chains,<sup>42–44</sup> and for particle-reinforced polymers.<sup>45–47</sup> Of course, the detailed nature of the polymer–filler interactions may be different for different systems. Nevertheless, the ambiguity in the results of Tsagaropoulos and Eisenberg further emphasizes the care which must be taken when interpreting glass transition behavior of filled polymers from viscoelastic data.

We conclude that for the materials studied herein, which had varying degrees of filler–polymer interactions, the polymer segmental motion, as determined using dynamic mechanical spectroscopy, is not significantly affected by filler reinforcement. Varying the particle surface area in carbon black-filled polybutadiene or changing the extent of chemical attachment of poly(styrene-*co*-butadiene) chains to silica particles does change the shape and magnitude of the  $\tan \delta$  vs temperature peak in the glass-to-rubber softening transition. However, this is due to changes in the small-strain rubbery response, arising primarily from the interparticle network. Proposed immobilized rubber or glassy shell concepts<sup>48–54</sup> do not appear to have much

relevance to the overall viscoelastic glass transition, at least for the two commercially important rubbers investigated in this study.

**Acknowledgment.** Bridgestone Americas is acknowledged for granting permission to publish this work. We thank the compounding and physical testing groups at the Bridgestone Americas Center for Research and Technology for their assistance. The work at the Naval Research Laboratory was supported by the Office of Naval Research.

## References and Notes

- (1) Alcoutlabi, M.; McKenna, G. B. *J. Phys.: Condens. Matter* **2005**, *17*, R461.
- (2) Tsagaropoulos, G.; Eisenberg, A. *Macromolecules* **1995**, *28*, 396.
- (3) Tsagaropoulos, G.; Eisenberg, A. *Macromolecules* **1995**, *28*, 6067.
- (4) Ferry, J. D. *Viscoelastic Properties of Polymers*; Wiley: New York, 1980.
- (5) Kraus, G.; Rollmann, K. W.; Gruver, J. T. *Macromolecules* **1970**, *3*, 92.
- (6) Iqbal, A.; Frommann, L.; Saleem, A.; Ishaq, M. *Polym. Compos.* **2007**, *28*, 186.
- (7) Kader, M. A.; Kim, K.; Lee, Y.-S.; Nah, C. *J. Mater. Sci.* **2006**, *41*, 7341.
- (8) Greenberg, A. R. *J. Mater. Sci. Lett.* **1987**, *6*, 78.
- (9) Gauthier, C.; Reynaud, E.; Vassolle, R.; Ladouce-Stelandre, L. *Polymer* **2004**, *45*, 2761.
- (10) Vieweg, S.; Unger, R.; Heinrich, G.; Donth, E. *J. Appl. Polym. Sci.* **1999**, *73*, 495.
- (11) Arrighi, V.; McEwen, I. J.; Qian, H.; Serrano Prieto, M. B. *Polymer* **2003**, *44*, 6259.
- (12) Lopez-Martinez, E. I.; Marquez-Lucero, A.; Hernandez-Escobar, C. A.; Flores-Gallardo, S. G.; Ibarra-Gomez, R.; Yacaman, M. J.; Zaragoza-Contreras, E. A. *J. Polym. Sci., Polym. Phys.* **2007**, *45*, 511.
- (13) Kraus, G.; Gruver, J. T. *J. Polym. Sci., Polym. Phys.* **1970**, *8*, 571.
- (14) Bogoslovov, R.; Roland, C. M.; Ellis, A. R.; Randall, A. M.; Robertson, C. G. *Macromolecules* **2008**, *41*, 1289.
- (15) Rittigstein, P.; Torkelson, J. M. *J. Polym. Sci., Polym. Phys.* **2006**, *44*, 2935.
- (16) Bansal, A.; Yang, H.; Li, C.; Benicewicz, B. C.; Kumar, S. K.; Schadler, L. S. *J. Polym. Sci., Polym. Phys.* **2006**, *44*, 2944.
- (17) Rodriguez, J. G. I.; Carreira, P.; Garcia-Diez, A.; Hui, D.; Artiaga, R.; Liz-Marzan, L. M. *J. Therm. Anal. Calorim.* **2007**, *87*, 45.
- (18) Metin, B.; Blum, F. D. *J. Chem. Phys.* **2006**, *125*, 054707.
- (19) O'Brien, J.; Cashell, E.; Wardell, G. E.; McBrierty, V. J. *Macromolecules* **1976**, *9*, 653.
- (20) Kenny, J. C.; McBrierty, V. J.; Rigbi, Z.; Douglass, D. C. *Macromolecules* **1991**, *24*, 436.
- (21) Kaufman, S.; Slichter, W. P.; Davis, D. D. *J. Polym. Sci., Polym. Phys.* **1971**, *9*, 829.
- (22) Fragiadakis, D.; Pissis, P.; Bokobza, L. *Polymer* **2005**, *46*, 6001.
- (23) Pissis, P.; Fragiadakis, D. *J. Macromol. Sci., Part B: Phys.* **2007**, *46*, 119.
- (24) Arrighi, V.; Higgins, J. S.; Burgess, A. H.; Floudas, G. *Polymer* **1998**, *39*, 6369.
- (25) Nakatani, A. I.; Ivkov, R.; Papanek, P.; Yang, H.; Gerspacher, M. *Rubber Chem. Technol.* **2000**, *73*, 847.
- (26) Gagliardi, S.; Arrighi, V.; Ferguson, R.; Telling, M. T. F. *Physica B: Condens. Matter* **2001**, *301*, 110.
- (27) Lee, K. J.; Lee, D. K.; Kim, Y. W.; Choe, W.-S.; Kim, J. H. *J. Polym. Sci., Polym. Phys.* **2007**, *45*, 2232.
- (28) Scurati, A.; Lin, C. J. *Rubber Chem. Technol.* **2006**, *79*, 170.
- (29) Schaefer, D. W.; Suryawanshi, C.; Pakdel, P.; Ilavsky, J.; Jemian, P. R. *Physica A* **2002**, *314*, 686.
- (30) Robertson, C. G.; Bogoslovov, R.; Roland, C. M. *Phys. Rev. E* **2007**, *75*, 051403.
- (31) Hess, W. M.; McDonald, G. C. *Rubber Chem. Technol.* **1983**, *56*, 892.
- (32) Wolff, S.; Wang, M.-J.; Tan, E.-H. *Rubber Chem. Technol.* **1993**, *66*, 163.
- (33) Meissner, B. *Rubber Chem. Technol.* **1995**, *68*, 297.
- (34) Payne, A. R. *J. Appl. Polym. Sci.* **1962**, *6*, 57.
- (35) Kraus, G. *J. Appl. Polym. Sci.: Appl. Polym. Symp.* **1984**, *39*, 75.
- (36) Robertson, C. G.; Wang, X. R. *Phys. Rev. Lett.* **2005**, *95*, 075703.
- (37) Ulmer, J. D. *Rubber Chem. Technol.* **1996**, *69*, 15.
- (38) Roland, C. M.; Lee, G. F. *Rubber Chem. Technol.* **1990**, *63*, 554.
- (39) Robertson, C. G.; Garcia-Franco, C. A.; Srinivas, S. *J. Polym. Sci., Polym. Phys.* **2004**, *42*, 1671.
- (40) Struglinski, M. J.; Graessley, W. W. *Macromolecules* **1985**, *18*–2630.
- (41) Kasehagen, L. J.; Macosko, C. W.; Trowbridge, D.; Magnus, F. *J. Rheol.* **1996**, *40*, 689.
- (42) Urayama, K.; Yokoyama, K.; Kohjiya, S. *Macromolecules* **2001**, *34*, 4513.
- (43) Ndoni, S.; Vorup, A.; Kramer, O. *Macromolecules* **1998**, *31*, 3353.
- (44) Kramer, O.; Greco, R.; Neira, R. A.; Ferry, J. D. *J. Polym. Sci., Polym. Phys.* **1974**, *12*, 2361.
- (45) Osman, M. A.; Atallah, A. *Polymer* **2006**, *47*, 2357.
- (46) Lobe, V. M.; White, J. L. *Polym. Eng. Sci.* **1979**, *19*, 617.
- (47) Zhu, Z.; Thompson, T.; Wang, S.-Q.; von Meerwall, E. D.; Halasa, A. *Macromolecules* **2005**, *38*, 8816.
- (48) Smit, P. P. A. *Rheol. Acta* **1966**, *5*, 277.
- (49) Struik, L. C. E. *Polymer* **1987**, *28*, 1534.
- (50) Wang, M.-J. *Rubber Chem. Technol.* **1998**, *71*, 520.
- (51) Berriot, J.; Montes, H.; Lequeux, F.; Long, D.; Sotta, P. *Macromolecules* **2002**, *35*, 9756.
- (52) Berriot, J.; Montes, H.; Lequeux, F.; Long, D.; Sotta, P. *Europhys. Lett.* **2003**, *64*, 50.
- (53) Montes, H.; Lequeux, F.; Berriot, J. *Macromolecules* **2003**, *36*, 8107.
- (54) Heinrich, G.; Kluppel, H. *Kautsch. Gummi Kunstst.* **2004**, *57*, 452.

MA7022364